



Contents lists available at ScienceDirect

Biochemical and Biophysical Research Communications

journal homepage: www.elsevier.com/locate/ybbrc

Mode of operation and low-resolution structure of a multi-domain and hyperthermophilic endo- β -1,3-glucanase from *Thermotoga petrophila*

Junio Cota^{a,d}, Thabata M. Alvarez^a, Ana P. Citadini^a, Camila Ramos Santos^b, Mario de Oliveira Neto^c, Renata R. Oliveira^b, Glauca M. Pastore^d, Roberto Ruller^a, Rolf A. Prade^e, Mario T. Murakami^b, Fabio M. Squina^{a,*}

^aLaboratório Nacional de Ciência e Tecnologia do Bioetanol (CTBE), do Centro Nacional de Pesquisa em Energia e Materiais, Campinas SP, Brazil

^bLaboratório Nacional de Biociências (LNBio), do Centro Nacional de Pesquisa em Energia e Materiais, Campinas SP, Brazil

^cInstituto de Física de São Carlos (IFSC), Universidade de São Paulo, São Carlos SP, Brazil

^dFaculdade de Engenharia de Alimentos (FEA), Universidade Estadual de Campinas, Campinas SP, Brazil

^eDepartment of Microbiology and Molecular Genetics, Oklahoma State University (OSU), Stillwater, OK, USA

ARTICLE INFO

Article history:

Received 16 February 2011

Available online 23 February 2011

Keywords:

Endo- β -1,3-glucanase

Glycoside hydrolase family 16

Hyperthermostable enzyme

Capillary zone electrophoresis

Small angle X-ray scattering

ABSTRACT

1,3- β -Glucan depolymerizing enzymes have considerable biotechnological applications including biofuel production, feedstock-chemicals and pharmaceuticals. Here we describe a comprehensive functional characterization and low-resolution structure of a hyperthermophilic laminarinase from *Thermotoga petrophila* (TpLam). We determine TpLam enzymatic mode of operation, which specifically cleaves internal β -1,3-glucosidic bonds. The enzyme most frequently attacks the bond between the 3rd and 4th residue from the non-reducing end, producing glucose, laminaribiose and laminaritriose as major products. Far-UV circular dichroism demonstrates that TpLam is formed mainly by beta structural elements, and the secondary structure is maintained after incubation at 90 °C. The structure resolved by small angle X-ray scattering, reveals a multi-domain structural architecture of a V-shape envelope with a catalytic domain flanked by two carbohydrate-binding modules.

Crown Copyright © 2011 Published by Elsevier Inc. All rights reserved.

1. Introduction

Renewable structural polysaccharides are abundant resources in the biosphere and represent a valuable industrial substrate for many industrial processes, such as biofuels production, feedstock-chemicals and pharmaceuticals [1]. β -1,3-Glucans are important polymers found mainly in yeast and filamentous fungi and are produced by plants (as callose) in response to tissue damage. This polymer is a major structural storage polysaccharide (laminarin) of the marine brown macro-algae of the genus *Laminaria*. β -1,3-glucan is also produced as insoluble exopolysaccharide by some fungal and bacterial species [2–5].

The β -1,3-glucanases are widely distributed among bacteria, fungi, and plants and are generally classified into two types, exo- β -1,3-glucanases (EC 3.2.1.58) and endo- β -1,3-glucanases (EC 3.2.1.6 and 3.2.1.39), which hydrolyze terminal or internal

glycoside linkages, respectively [28]. These enzymes are further classified as family members (GH) 16, 17, 55, 64, and 81 of the CaZy system, which is based on structural similarities of the amino acid sequence [28]. However, CaZy GH families display a dispersed range of enzymatic activity, and updating biochemical and biophysical information strengthens the CaZy purpose.

To date, crystal structures from family GH 16 endo- β -1,3-glucanases (3.2.1.39) have been determined for *Pyrococcus furiosus* [6], *Rhodothermus marinus* [6], *Streptomyces sioyaensis* [7], and *Nocardiopsis sp* [8]. The active site region of family GH16 consists of three acidic residues, two glutamic and one aspartic acid in the active site, and two conserved tryptophan residues, which promote substrate binding and transition-state stabilization [9]. The overall fold of these enzymes consists of a classical sandwich-like β -jelly-roll motif formed by the face-to-face packing of two antiparallel sheets containing seven and eight strands with a deep cavity [6–8,10].

In this work is reported a comprehensive functional characterization of an endo- β -1,3-glucanase from *Thermotoga petrophila* (TpLam), including a detailed description of the hydrolytic mode of operation, along with structural insights of this hyperthermostable enzyme.

* Corresponding author. Address: Rua Giuseppe Máximo Scolfaro, 10.000 Polo II de Alta Tecnologia, Caixa Postal 6170, Campinas, SP 13083-970, Brazil. Fax: +55 19 35183104.

E-mail address: fabio.squina@bioetanol.org.br (F.M. Squina).

2. Material and methods

2.1. Cloning and purification of TpLam

The full-length coding TpLam gene (Tpet_0899) derived from genomic DNA of *T. petrophila* was amplified by standard PCR method for cloning the mature enzyme without signal peptide. The primer set used for amplification was 5'-GCTAGCCAAAACATCCTTGCAACGC-3' and 5'-GGATCCTCATTGAGGACTCACCGAAA-3', and the gene segment was cloned into the pET28a (Novagen) vector using *NheI* and *BamHI* restriction sites. The protein expression and purification steps, included a Ni²⁺-chelating affinity and size-exclusion chromatography, were performed following Squina et al., 2010 [11]. The purified TpLam was further analyzed by SDS-PAGE. Protein concentration was determined by Bradford method.

2.2. Enzyme characterization

Standard enzymatic assays for TpLam evaluation were performed following previous work [29]. The determination of the optimum pH and temperature profiles, thermo stability evaluation and 8-aminopyreno-1,3,6-trisulfonic acid (APTS) labeling was performed as described previously [28]. The mixture was incubated at 90 °C for 10 min in standard assays with laminarin or 60 min aiming at to determine the specific activity in a set of polysaccharides (purchased from the best source possible, Sigma Aldrich and Megazyme). The enzymatic activity and substrate specificity were determined from the amount of reducing sugar liberated from different polysaccharide substrates by the DNS method [12]. One unit of enzyme was defined as the quantity of enzyme that released reducing sugars at rate of 1 μmol/min. The kinetic parameters for TpLam activity were estimated from initial rates at twelve substrates concentration in the 1.6–65 mg/mL range in standard assay.

A Response Surface Methodology was performed to optimize the reaction conditions for TpLam. The variables analyzed here were the pH together with temperature, whereas a Central Composite Design ($k = 2$) with four central points totalizing 12 experiments (Table 1) was considered for optimization of these variables. Details concerning the statistical approaches for these experiments can be found in Myers and Montgomery [13] and all β-1,3-glucanase activity assays were carried out following our previous work using laminarin as substrate (stock 0,5% in water) [14,15].

Capillary electrophoresis of oligosaccharides and Far-UV circular dichroism (CD) measurements (190–260 nm) and prediction of secondary structure from the dichroism circular spectrum was conducted as described as previously [14–16].

Table 1
Central composite design matrix (22) and the response of TpLam activity after 10 min of incubation.

Run no.	Coded levels ($X_1 = \text{pH}; X_2 = T$)		Actual levels ($X_1 = \text{pH}; X_2 = T$)		Laminarinase activity (IU/mg protein)
	X_1	X_2	X_1	X_2	
1	-1	-1	4.6	74.2	139,8
2	1	-1	7.4	74.2	170,9
3	-1	1	4.6	94.8	175,2
4	1	1	7.4	94.8	204,2
5	-1.414	0	4.0	84.5	68,6
6	1.414	0	8.0	84.5	154,6
7	0	-1.414	6.0	70.0	159,7
8	0	1.414	6.0	99.0	238,9
9	0	0	6.0	84.5	234,6
10	0	0	6.0	84.5	241,3
11	0	0	6.0	84.5	247,8
12	0	0	6.0	84.5	247,1

2.3. Small angle X-ray scattering

Small Angle X-ray Scattering (SAXS) data for TpLam at the concentrations 4 and 8 mg/mL were collected on the SAXS2 beam line at the Brazilian Synchrotron Light Laboratory. The radiation wavelength was set to 1.48 Å and a 165 mm MarCCD detector was used to record the scattering patterns. The sample-to-detector distance was set to 1022.5 mm to give a scattering vector-range from 0.013 to 0.33 nm⁻¹, where q is the magnitude of the q-vector defined by $q = 4\pi/\lambda \sin\theta$ (2θ is the scattering angle). Protein samples were prepared in 20 mM phosphate 50 mM NaCl buffer pH 6.0. The integration of SAXS patterns were performed using Fit2D software [17] and the curves were scaled by protein concentration. The radius of gyration (R_g) was approximated using two independent procedures, by Guinier equation [18] and by indirect Fourier transform method using GNOM program [18]. The distance distribution functions $p(r)$ also was evaluated by GNOM and the maximum diameter (D_{max}) was obtained. Molecular weight was calculated using the procedure implemented on web tool SAXSmow [19]. Dummy atom model (DAMs) was calculated from the experimental SAXS data using *ab initio* procedure implemented in Dammin program [20]. Several runs of *ab initio* shape determination with different starting conditions led to consistent results as judged by the structural similarity of the output models, yielding nearly identical scattering patterns and fitting statistics in a stable and self-consistent process. CRY SOL program calculated the simulated scattering curve from DAM and homology model [21]. The evaluation of R_g and D_{max} were performed with the same program.

2.4. Homology molecular modeling

Homology models for each domain of TpLam were constructed using the HHPred server [22]. These models were renumbered according to the wild protein and spatially disposed in this order: 1, 2, and 3, in a manner to avoid clashes, with MASSHA [23]. CRY SOL program calculated the of the scattering amplitudes for atoms, excluded volume and border for each model and it was input for the next approach [24]. BUNCH software, which employs rigid body model (RBM) and simulated annealing routines, was used to find the best relative positions of the high-resolution models [25]. This solution was superposed in the DAM with SUPCOMB [25].

3. Results and discussion

3.1. TpLam is a specific endo β-1-3 acting glucanase with remarkable thermostable properties

TpLam activity was investigated at different pH values and temperatures. The enzyme exhibited at least 80% of its optimal activity over a pH range, from 5 to 7 (data not shown), which resemble other hyperthermophilic laminarinases [2,26]. Purified TpLam showed a relative activity ranging from 82% to 86% at temperatures of 78 °C and 95 °C and pH 6, respectively (data not shown). A Central Composite Design with two variables was performed to optimize reaction conditions. The model (Fig. 1A and B) was validated by an analysis of variance (ANOVA) showing that the model was significant at high confidence level (95%), with $R^2 = 0.96$. The best condition for enzyme activity was reached at pH 6.2 and 91 °C. To validate the model, at pH 6 and temperature of 91 °C the predicted laminarinase activity of 250.0 IU/mg protein, whereas experimentally determined was 260.8 IU/mg protein. TpLam was heat-stable at 70 °C and maintained 60% of residual activity after 16 h at 80 °C. The enzyme showed a half-life time of 577 and 126 min at 90 and 95 °C, respectively (Fig. 1C). The

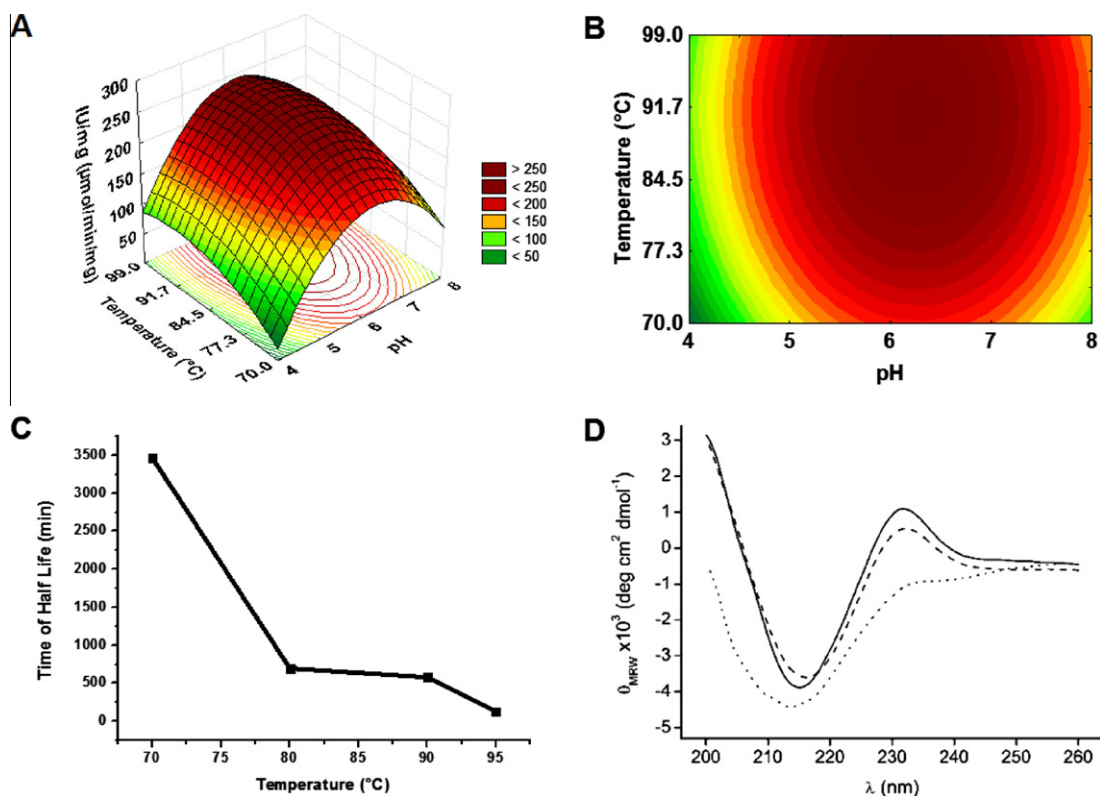


Fig. 1. Response surface (A) and contour plot (B) for the influence of temperature and pH on TpLam activity. (C) Curve of decay of time of half life ($t_{1/2}$) using four different temperatures (70, 80, 90, and 95 °C). (D) Thermal stability of laminarinase analyzed by circular dichroism. CD spectra were taken at 20 °C (solid line) and after 18 h at 90 °C.

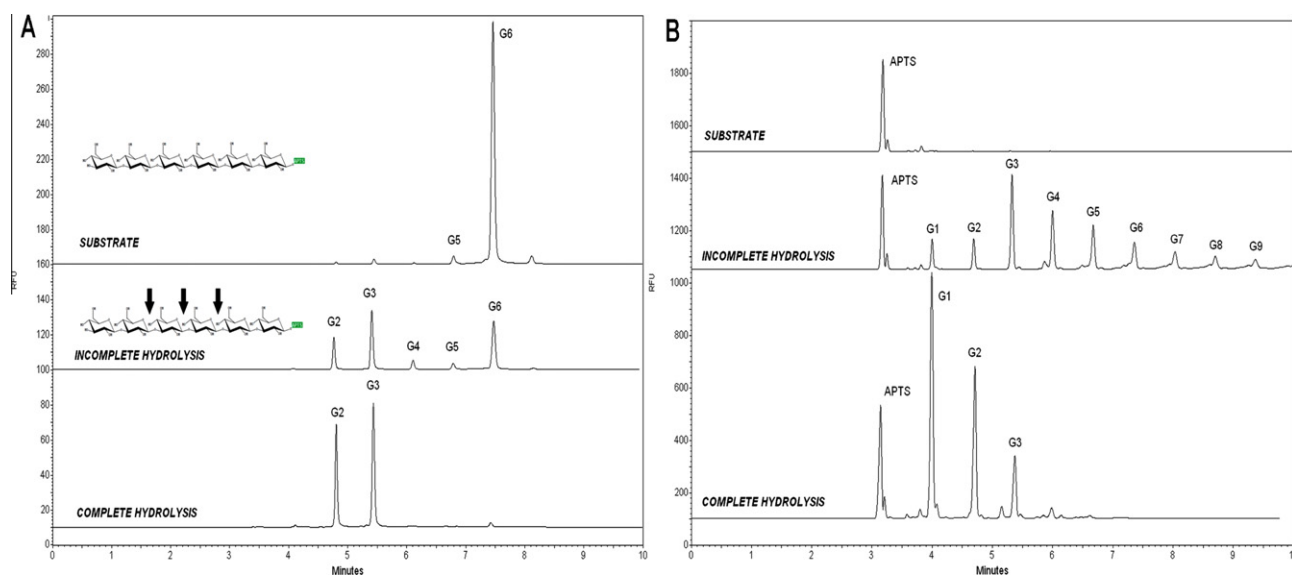


Fig. 2. Capillary zone electrophoresis of APTS-labeled oligosaccharides. (A) Incomplete and complete hydrolysis of APTS-reducing-end-labeled-laminarihexaose. (B) Incomplete and complete hydrolysis of laminarin (APTS-labeled after the enzymatic reaction). G1, G2, G3, G4, G5, G6, G7, G8, and G9 indicate the degree of polymerization of glucose oligomers.

optimum temperature reported for the TpLam is comparable to other thermophilic bacterial endo- β -1,3-glucanases from *T. neapolitana* and *P. furiosus*, which display temperatures of 95 °C and 100 °C, respectively [2,26].

The recombinant enzyme was highly specific on β 1–3-linked polysaccharides, such as laminarin (48.07 IU/mg) and β -glucan from barley (41.55 IU/mg) and lichenan (21.37 IU/mg). No β 1–4

glucanase activity was detected, based on enzymatic assays using avicel, carboxymethylcellulose and cellopentaose, as well as xylan, arabinan and manan containing polysaccharides. Kinetic values were determined experimentally from the initial rates of laminarin hydrolysis at each substrate concentration and standard assay conditions. A V_{max} of 558.2 μ mol/min/mg and a K_m of 3.3 mg/mL were found for purified TpLam. Two other kinetic constants were

determined from the experimental data and the values for catalytic constant (K_{cat}) and K_{cat}/K_m were 680.3 s^{-1} and 206.2, respectively.

The CD spectrum of native laminarinase presents a negative peak at 217 nm and a positive peak at 232 nm (Fig. 1D). The 217 nm peak is characteristic of β -structures and the 232 nm peak is explained by the aromatic residues contribution. All domains have a high content of beta-sheet, with few α -helical structures. Glycoside hydrolases are rich in aromatic residues, which are notably important to form the active site pocket and to interact with the substrate. Those side chains contribute to the CD spectrum, especially in proteins of low α -helix content, such as the laminarinase, giving positive bands in the 220–230 region [27]. At 90 °C little change is observed in the CD spectrum of laminarinase, showing its stability in terms of secondary structure (Fig. 1D). After incubation at 90 °C for 18 h, CD spectrum was changed with the loss of the 232 nm peak indicating protein unfolding (Fig. 1D). Enzymatic assays demonstrated its inactivation under such conditions, which confirmed CD analysis.

Capillary zone electrophoresis analysis of the corresponding hydrolysis products was performed in an attempt to define the

Table 2

Structural parameters derived from SAXS data for TpLam.

Parameters/Sample	Exp ^a		DAM ^b	RBM ^c
D_{max} (Å)	130.0 ± 5.0		130.8	135.3
R_g (Å)	40.10 (Guinier)	42.0 ± 0.1 (GNOM)	41.99	42.20
Resolution (Å)	19.0		19.0	–
MW_{SAXS} (kDa)	67.9		–	–

Resolution: $2\pi/q$.

^a Calculated from the experimental data at 4 mg/mL.

^b Calculated from dummy atom model.

^c Calculated from rigid body model (RBM), BUNCH program.

mode of action for TpLam. During the course of hydrolysis of APTS-labeled laminarihexaose (non-reducing end available) the enzyme most likely attacks the internal glycosidic linkages releasing fluorescent dimers, trimers and tetramers (Fig. 2A). Final hydrolysis products were dimers and trimers, suggesting that they cannot be degraded further (Fig. 2A). Nevertheless through APTS-labeling (after the enzymatic reaction) of hydrolysis products from laminarihexaose showed formation of glucose (data not shown). Using natural laminarin the degradation pattern was characteristic for endoglucanases (APTS-labeled after the reaction) with production of intermediates with different degree of polymerization (Fig. 2B), yielding as final products; glucose, laminaribiose and laminaritriose (Fig. 2B).

3.2. Low-resolution structure of TpLam reveals a multi-domain V-shape conformation

The structural parameters derived from experimental curve, DAM and RBM are shown in Table 2. The values obtained from these different calculations are similar, indicating an agreement among the SAXS data, the SAXS-derived envelope and the RBM. Moreover, these data indicate that the maximum intra particle distance (D_{max}) and R_g of TpLam are 130 and 42 Å, respectively, meaning that the D_{max} is three times greater than the R_g , and the particle should have an elongated form.

The scattering curve, the distance distribution function and the low-resolution structure are shown in Fig. 3A. As expected, the DAM is elongated, exhibiting a V-shape with two asymmetric arms. The three-domain high-resolution model was well fitted into the DAM with the catalytic core (CC2) occupying the central region and two carbohydrate-binding modules (CBM) forming the arms. The asymmetry of the molecule is due to the fact that the linker

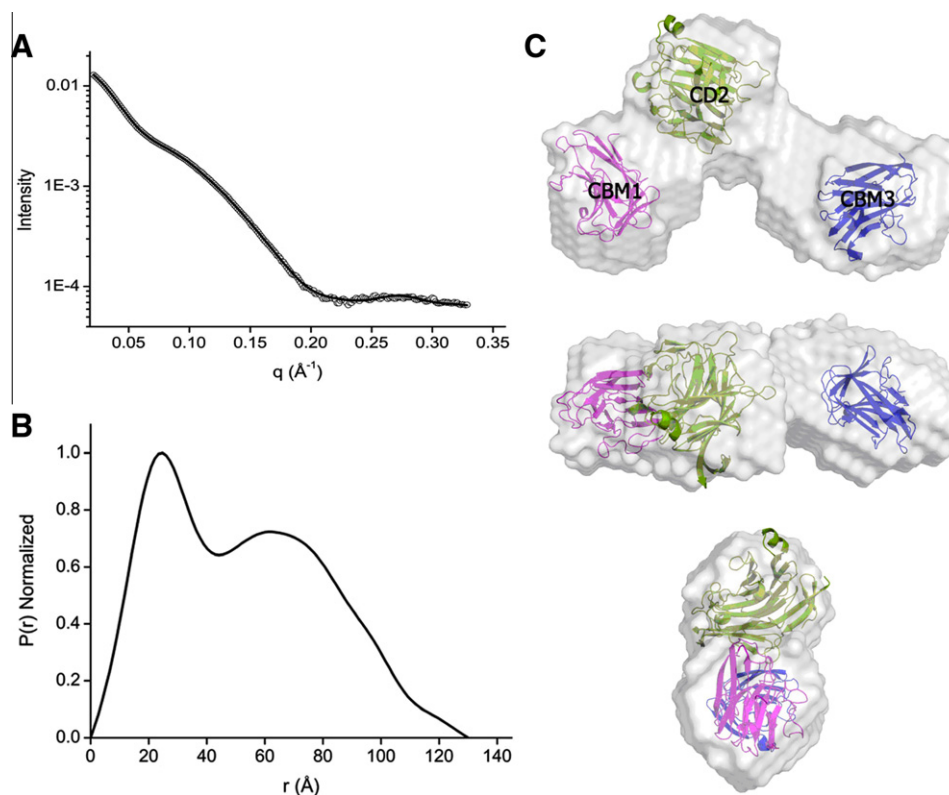


Fig. 3. Laminarinase analysis by SAXS. (A) Experimental scattering curve (open circles) and fit produced by GNOM (solid line). (B) Distance distribution function computed from the experimental data. (C) Laminarinase model with CBM1 (magenta), CD2 (green) and CBM3 (blue) domains fitted into the envelope obtained from SAXS data is shown in different orientations. (For interpretation of the references to colour in this figure legend, the reader is referred to the web version of this article.)

between CC2 and CBM3 (residues 459–486) is longer than the linker between CBM1 and CC2 (residues 187–199). This feature enables unambiguously to distinct the correct location of N- and C-terminal CBM domains. Moreover, the linkers could act as hinges permitting conformational changes required for substrate recognition and catalysis. This mobility is particularly evident in the CBM3-containing arm in the SAXS model, where the average of different positions resulted in a larger volume than expected from the high-resolution model.

In conclusion, we evaluated the TpLam a specific endo β -1–3 acting glucanase with remarkable thermostable properties. The study herein depicted enzymatic mode of attack, performed a comprehensive spectrometric analysis of hyperthermophilicity and determined the low-resolution structure of a multi-domain V-shape enzyme bearing two carbohydrate-binding modules. Our findings provide biochemical and structural basis for further studies of endo- β -1,3-glucanases, which are important components of enzymatic repertory in polysaccharide degradation with many biotechnological applications.

Acknowledgments

This research was supported by grants from FAPESP (08/58037-9) to FMS and CNPq (478059/2009-4) to MTM and scholarship from CNPq (140420/2009-6) to JC.

References

- [1] M.E. Himmel, S.Y. Ding, D.K. Johnson, et al., Biomass recalcitrance. Engineering plants and enzymes for biofuels production, *Science* 315 (2007) 804–807.
- [2] V.V. Zverlov, I.Y. Volkov, T.V. Velikodvorskaya, W.H. Schwarz, Highly thermostable endo-1, 3-beta-glucanase (laminarinase) LamA from *Thermotoga neapolitana*: nucleotide sequence of the gene and characterization of the recombinant gene product, *Microbiology* 143 (1997) 1701–1708.
- [3] J. Vasur, R. Kawai, E. Andersson, et al., X-ray crystal structures of *Phanerochaete chrysosporium* Laminarinase 16A in complex with products from lichenin and laminarin hydrolysis, *FEBS J.* 276 (2007) 3858–3869.
- [4] T.R. Storseth, K. Hansen, K.I. Reitan, J. Skjermo, *Carbohydr. Res.* 340 (2005) 1159–1164.
- [5] M. Hrmova, G.B. Fincher, Purification and properties of three (1-3)-beta-D-glucanase isoenzymes from young leaves of barley (*Hordeum vulgare*), *Biochem. J.* (1993) 453–461.
- [6] A. Ilari, A. Fiorillo, S. Angelaccio, et al., Crystal structure of a family 16 endoglucanase from the hyperthermophile *Pyrococcus furiosus*—structural basis of substrate recognition, *FEBS J.* 276 (2009) 1048–1058.
- [7] T.Y. Hong, Y.T. Hsiao, M. Meng, T.T. Li, The 1.5 Å structure of endo-1, 3-beta-glucanase from *Streptomyces sioyaensis*: evolution of the active-site structure for 1, 3-beta-glucan-binding specificity and hydrolysis *Acta Crystallogr., D Biol. Crystallogr.* 64 (2008) 964–970.
- [8] G. Fibriansah, S. Masuda, N. Koizumi, et al., The 1.3 Å crystal structure of a novel endo-beta-1, 3-glucanase of glycoside hydrolase family 16 from alkaliphilic *Nocardiopsis* sp. strain F96, *Proteins* 69 (2007) 683–690.
- [9] O.J. Gaiser, K. Piotukh, M.N. Ponnuswamy, et al., Structural basis for the substrate specificity of a *Bacillus* 1, 3–1, 4-beta-glucanase, *J. Mol. Biol.* 357 (2006) 1211–1225.
- [10] M. Krah, R. Misselwitz, O. Politz, et al., The laminarinase from thermophilic eubacterium *Rhodothermus marinus* conformation, Stability, and identification of active site carboxylic residues by site-directed mutagenesis, *Eur. J. Biochem.* 257 (1998) 101–111.
- [11] F.M. Squina, C.R. Santos, D.A. Ribeiro, et al., Substrate cleavage pattern, biophysical characterization and low-resolution structure of a novel hyperthermostable arabinanase from *Thermotoga petrophila*, *Biochem. Biophys. Res. Com.* 399 (2010) 505–511.
- [12] G.L. Miller, Use of dinitrosalicylic acid reagent for determination of reducing sugar, *Anal. Chem.* 31 (1959) 426–428.
- [13] R.H. Myers, D.C. Montgomery, *Response Surface Methodology*, second ed., John Wiley & Sons, New York, 2001.
- [14] C.R. Santos, F.M. Squina, A.M. Navarro, et al., Functional and biophysical characterization of a hyperthermostable GH51 alpha-L-arabinofuranosidase from *Thermotoga petrophila*, *Biotech. Lett.* 33 (2010) 131–137.
- [15] C.R. Santos, A.N. Meza, Z.B. Hoffmann, et al., Thermal-induced conformational changes in the product release area drive the enzymatic activity of xylanases 10B: Crystal structure, conformational stability and functional characterization of the xylanase 10B from *Thermotoga petrophila* RKU-1, *Biochem. Biophys. Res. Com.* 403 (2010) 214–219.
- [16] A. Lobley, L. Whitmore, B.A. Wallace, DICHROWEB: an interactive website for the analysis of protein secondary structure from circular dichroism spectra, *Bioinformatics* 18 (2002) 211–212.
- [17] A. P. Hammersley, FIT2D: An Introduction and Overview. In ESRF Internal Report, (1997).
- [18] A. Guinier, G. Fournet, *Small-Angle Scattering of X-Rays*, John Wiley and Sons, New York, 1955.
- [19] H. Fischer, M. Oliveira Neto, H.B. Napolitano, et al., Determination of the molecular weight of proteins in solution from a single small-angle X-ray scattering measurement on a relative scale, *J. Appl. Cryst.* 43 (2010) 101–109.
- [20] D.I. Svergun, Determination of the regularization parameter in indirect-transform methods using perceptual criteria, *J. Appl. Cryst.* 25 (1992) 495–503.
- [21] D.I. Svergun, Restoring low resolution structure of biological macromolecules from solution scattering using simulated annealing, *Biophys. J.* 76 (1999) 2879–2886.
- [22] J. Söding, A. Biegert, A.N. Lupas, The HHpred interactive server, *Nucleic Acids Res.* 33 (2005) W244–W248.
- [23] P.V. Konarev, M.V. Petoukhov, D.I. Svergun, MASSHA - a graphics system for rigid-body modeling of macromolecular complexes against solution scattering data, *J. Appl. Crystallogr.* 34 (2001) 527–532.
- [24] D.I. Svergun, C. Barberato, M.H.J. Koch, CRYSOLO - a program to evaluate X-ray solution scattering of biological macromolecules from atomic coordinates, *J. Appl. Crystallogr.* 28 (1995) 768–773.
- [25] M.V. Petoukhov, D.I. Svergun, Global rigid body modeling of macromolecular complexes against small-angle scattering data, *Biophys. J.* 89 (2005) 1237–1250.
- [26] Y. Gueguen, W.G.B. Voorhorst, J. van der Oost, W.M. de Vos, Molecular and biochemical characterization of an endo- β -1, 3-glucanase of the *Hyperthermophilic archaeon Pyrococcus furiosus*, *J. Biol. Chem.* 272 (1997) 31258–31264.
- [27] R.W. Woody, Contributions of tryptophan side chains to the far-ultraviolet circular dichroism of proteins, *Eur. Biophys. J.* 23 (1994) 253–262.
- [28] B.L. Cantarel, P.M. Coutinho, C. Rancurel, et al., The Carbohydrate-Active EnZymes database (CAZy): an expert resource for Glycogenomics, *Nucleic Acids Res.* 37 (2009) D233–D238.
- [29] F.M. Squina, A.J. Mort, S.R. Decker, et al., Xylan decomposition by *Aspergillus clavatus* endo-xylanase, *Protein Expression Purif.* 68 (2009) 65–71.